ChemPubSoc Europe

DOI: 10.1002/chem.201803521

CHEMISTRY A European Journal Communicatio

Antitumor Agents

Highly Charged, Cytotoxic, Cyclometalated Iridium(III) Complexes as Cancer Stem Cell Mitochondriotropics

Kristine Laws,[a] Arvin Eskandari,[a] Chunxin Lu,[a, b] and Kogularamanan Suntharalingam*[a]

Abstract: The cancer stem cell (CSC) toxicity and mechanism of action of a series of iridium(III) complexes bearing polypridyl and charged 1-methyl-2-(2-pyridyl)pyridinium ligands, **1**–**4** is reported. The most effective complex (containing 1,10-phenanthroline), **3**, kills CSCs and bulk cancer cells with equal potency (in the micromolar range), indicating that it could potentially remove heterogenous tumour populations with a single dose. Encouragingly, **3** also inhibits mammopshere formation to a similar extent as salinomycin, a well-established anti-CSC agent. This complex induces CSC apoptosis by mitochondrial membrane depolarization, inhibition of mitochondrial metabolism, and intracellular reactive oxygen species (ROS) generation. To the best of our knowledge, this is the first study to investigate the anti-CSC properties of iridium complexes.

Cancer stem cells (CSCs) are a radiotherapy and chemotherapy resistant subset of tumour cells found in many solid cancers and leukaemias.[1] CSCs are believed to be partly responsible for cancer relapse due to their inherent ability to initiate tumours and promote metastasis.[2] Current cancer therapies work by removing bulk cancer cells, however, they are unable to remove CSCs, which remain untouched and can seed secondary tumour growth.[3] Given the clinical implications of CSCs it is imperative that future cancer therapies have the ability to remove bulk cancer cells and CSCs, so the possibility of cancer reoccurrence is diminished. Certain CSC traits have been recognised as potential therapeutic targets such as overexpressed cell surface proteins, deregulated cell signalling pathways, and components within the CSC microenvironment; nevertheless, a clinically effective anti-CSC agent remains elusive.[4] Recent studies on lung and breast cancer, and leukaemia populations revealed that some mitochondrial features were distinctly different in CSCs compared to the bulk tumour populations.[5] These include, but are not limited to, mitochondrial DNA content, metabolic phenotype, intracellular ATP, reactive oxygen species (ROS) level, and mitochondrial membrane potential. Furthermore, independent studies showed that CSCs have a higher mitochondrial mass than bulk cancer cells, highlighting the significance of mitochondrial function to CSC regulation.[6] Therefore, mitochondrial targeting could offer a viable approach to remove CSCs. We recently reported a metallopeptide containing dichloro(1,10-phenanthroline) copper(II), a ROS-generating CSC-potent complex, affixed to an established mitochondrial-penetrating peptides (MPPs), capable of selectively killing breast CSCs over bulk breast cancer cells through mitochondrial dysfunction.[7] Although this metallopeptide exhibited promising in vitro CSC potency, potential in vivo application is limited by the high reactivity of the copper(II)-phenanthroline warhead, and akin to other peptide-based chemotherapeutics, challenges relating to pharmacokinetics and clearance.[8] Targeting CSC mitochondria using chemically inert small molecules could be a more effective and translatable strategy.

Several iridium complexes possess impressive anticancer properties.[9] Of note, organometallic iridium(III) complexes bearing electron-rich pentamethylcyclopentadienyl ligands display promising potency against various cancer cell types (up to sub-micromolar).[10] Organometallic iridium(III) complexes with pyridocarbazole exhibit antiangiogenicity in vivo (zebrafish models) and photocytotoxicity against bulk cancer cells.[11] Cyclometalated iridium(III) complexes with polypridyl ligands have attracted a lot of attention as therapeutic and diagnostic tools over the last decade, due to their high stability (low spin, d^6) and rich phosphorescent properties.[12] Certain cyclometalated iridium(III) complexes also act as effective photoinduced singlet oxygen producers in bulk cancer cells.[13] According to the large body of work already published on the anticancer properties of iridium(III) complexes, the cell toxicity and associated mechanism of action is highly dependent on the coordinating ligands.[14] The coordinating ligands also dictate intracellular localization, with bulky, lipophilic ligands promoting mitochondrial accumulation.[15] Mitochondrial targeting is generally achieved by lipophilic ($\log P > -1.7$) and cationic ($Z > 0$) species.[16] Here, we have sought to exploit these determinants to develop a series of intrinsically inert, lipophilic, and cationic cyclometalated iridium(III) complexes that can target and disrupt mitochondrial function in breast CSCs. Specifically, we present cyclometalated iridium(III) complexes with two charged 1-methyl-2-(2-pyridyl)pyridinium ligands and a lipophilic polypyridine ligand, with an overall +3 charge. As certain CSCs have a higher mitochondrial load than bulk cancer cells and normal

[a] K. Laws, A. Eskandari, Dr. C. Lu, Dr. K. Suntharalingam
Department of Chemistry, King's College London, London SE1 1DB (UK)
E-mail: kogularamanan.suntharalingam@kcl.ac.uk

[b] Dr. C. Lu
College of Biological, Chemical Sciences and Engineering
Jiaxing University, Jiaxing 314001 (China)

Supporting information and the ORCID identification number(s) for the author(s) of this article can be found under: https://doi.org/10.1002/chem.201803521.

cells, compounds that can target mitochondria, such as the cationic iridium(III) complexes presented here, have the potential to kill mitochondria-rich CSCs effectively.

The cyclometalated iridium(III) complexes, **1**–**4** (Figure 1 A) used in this study were synthesised by refluxing $[\{Ir(\mu\text{-}Cl)(1\text{-methyl-2-(2-pyridyl)pyridinium})_2\}_2][PF_6]_4$ with >3 equiv of the

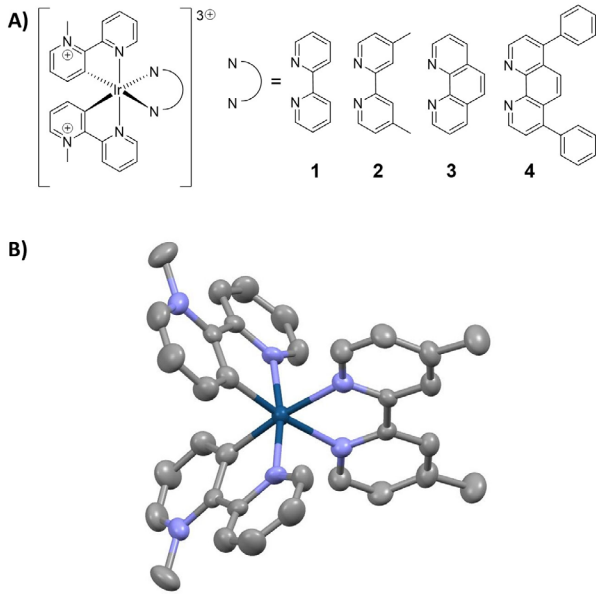

Figure 1. (A) Chemical structures of the cyclometalated iridium(III) complexes, **1**–**4** investigated in this study. The charged iridium(III) complexes were all isolated as hexafluorophosphate salts. (B) X-ray structure of **2**. Ellipsoids are shown at 50% probability, C in grey, N in light blue, and Ir in dark blue. H atoms and hexafluorophosphate counter anions have been omitted for clarity.

appropriate polypyridine ligand (2,2′-bipyridine, 4,4′-dimethyl-2,2′-bipyridine, 1,10-phenanthroline, or 4,7-diphenyl-1,10-phenanthroline) and >2 equiv of $AgPF_6$ in 2-methoxyethanol/water (2:1) for 3–5 days under nitrogen. Upon work up by Celite filtration, evaporation and anion exchange using NBu_4Cl or NaCl, the resultant solids were purified by Sephadex column using 0.012 mM NaCl acetone/water (1:1) solution and subsequently converted to the corresponding hexafluorophosphate salt. The iridium(III) complexes, **1**–**4** isolated as yellow solids, were characterised by ^{1}H NMR, ^{13}C NMR, high-resolution ESI mass spectrometry, IR spectroscopy, elemental analysis and X-ray crystallography (for **2**) (see the Supporting Information, Figures S1–S4, CCDC 1836118).[25] Distinctive molecular ion peaks corresponding to **1**–**4** with the appropriate isotopic pattern were observed in the ESI mass spectra (m/z = 979.1384 a.m.u, $[\mathbf{1}\text{-}PF_6]^+$; 1007.1726 a.m.u, $[\mathbf{2}\text{-}PF_6]^+$; 237.7271 a.m.u, $[\mathbf{3}\text{-}3PF_6]^{3+}$; 1155.2108 a.m.u, $[\mathbf{4}\text{-}PF_6]^+$) (Figures S5–S8, Supporting Information), confirming formation of the desired products. The purity of **1**–**4** was established by elemental analysis. The structure of **2** was further confirmed by X-ray diffraction studies and is depicted in Figure 1 B. Crystals of **2** suitable for an X-ray diffraction analysis were obtained by slow diffusion of diethyl ether into a concentrated acetonitrile solution of **2** (Table S1, Supporting Information). Selected bond lengths and bond angle data are presented in Table S2. The complex exhibits a distorted octahedral geometry with the iridium centre coordinated to two 1-methyl-2-(2-pyridyl)pyridinium ligands and one 4,4′-dimethyl-2,2′-bipyridine ligand, each forming a five-membered chelated ring. The average Ir–C (2.011 Å) bond length is consistent with bond parameters for related octahedral iridium(III) complexes.[17] As expected, the Ir–N (2.136 Å) bonds *trans* to the cyclometalated bonds are longer than the Ir–N bonds (2.056 Å) in the *cis* position.

The photophysical properties of **1**–**4** were studied in acetonitrile, dichloromethane, water, and PBS and are summarised in Table 1 and Tables S3 and S4 (also see Figures S9–S16 in the Supporting Information). The iridium(III) complexes, **1**–**4** displayed intense absorption bands between 250 and 300 nm,

Table 1. Absorbance, emission (λ_{ex} = 450 nm), lifetime and quantum yield data for **1**–**4** (50 μM) in acetonitrile.

Compound	λ_{max}[nm] (ε [$M^{-1}cm^{-1}$])	λ_{em} [nm]	τ [μs]	Φ [%]
1	223 (42777), 255 (17218), 298 (16803), 312 (14083), 356 (4912), 443 (1223)	527, 553	1.79	11.5
2	234 (45490), 257 (32653), 298 (31838), 311 (27762), 356 (8755), 446 (1951)	530, 558	1.86	13.9
3	226 (85122), 270 (69144), 290 (43333), 354 (11000), 442 (2624)	528, 549	2.15	17.3
4	223 (84811), 288 (56900), 378 (10700), 445 (2110)	528, 553	2.08	22.5

which are tentatively assigned to π–π* and high energy metal-to-ligand charge-transfer (MLCT) transitions involving both the 1-methyl-2-(2-pyridyl)pyridinium and corresponding polypyridine ligands. Weaker bands between 350 and 450 nm are assigned largely to MLCT (d–π*) transitions involving the 1-methyl-2-(2-pyridyl)pyridinium ligand. The iridium(III) complexes, **1**–**4** exhibited green emission comprising of two broad signals, upon excitation at 450 nm. The bands at 524–532 nm and 548–560 nm correspond to ^{3}LC (associated to the 1-methyl-2-(2-pyridyl)pyridinium ligand) and ^{3}MLCT transitions, respectively. Solvent polarity (water/PBS > acetonitrile > dichloromethane) has a minor effect on emission wavelength, but significantly influences emission intensity. All of the complexes have emission lifetimes in the microsecond region, ranging from 1.79–2.08 μs (in acetonitrile) with mono-exponen-

tial decay kinetics (Figure S17), suggesting that emission originates from a triplet excited state. The quantum yield, Φ (in acetonitrile) of the iridium(III) complexes increases in the following order; **1** (11.5%) < **2** (13.9%) < **3** (17.3%) < **4** (22.5%), and is consistent with those reported for similar complexes (Figure S18).[17b]

The lipophilicity of **1**–**4** was determined by measuring the extent to which it partitioned between octanol and water, *P*. The experimentally determined Log*P* values of **1**–**4** varied from −0.86 to −1.42 (Table S5). The Log*P* values of **1**–**4** are consistent with other mitochondriotropics (Log*P* > −1.7), suggesting that the iridium(III) complexes should be readily taken up by cells and enter the mitochondrial matrix.[16, 18] UV/Vis and high-resolution ESI mass spectroscopy studies were carried out to assess the stability of **3** and **4**, taken as representative members of the iridium(III) series, in biologically relevant solutions. The UV/Vis π–π* and MLCT absorption bands of **3** and **4** (50 μM) in PBS:DMSO (200:1) remained unchanged over 24 h at 37 °C (Figures S19 and S20). In PBS:DMSO (200:1) containing 5 equiv of ascorbic acid or glutathione, the UV/Vis absorption of **3** and **4** (50 μM) remained unaltered over 24 h at 37 °C (Figures S21–S24). Under these conditions, peaks corresponding to the molecular ion of **3** and **4** with the expected isotopic distribution (m/z = 1003.1290 a.m.u, [**3**-PF_6]$^+$; 1155.2111 a.m.u, [**4**-PF_6]$^+$) were observed in the positive mode of the ESI mass spectrum (Figures S25 and S26). Collectively, this suggests that the iridium complexes are stable and remain intact under biologically reducing conditions. Before carrying out cellular studies, the stability of **1**–**4** in mammary epithelial cell growth medium (MEGM) was investigated (Figures S27–S30). The UV/Vis trace of **1**–**4** (50 μM) in MEGM/DMSO (200:1) displayed no changes after incubation at 37 °C for 24 hours. Therefore **1**–**4** were deemed stable for cellular studies.

The cytotoxicity of **1**–**4** against bulk bone (U2OS), liver (HepG2), and breast (HMLER) cancer cells, and breast CSC-enriched cells (HMLER-shEcad) was determined using the MTT assay. The IC_{50} values were determined from dose–response curves (Figures S31–S34) and are summarised in Table 2. The 1,10-phenanthroline- and 4,7-diphenyl-1,10-phenanthroline-bearing complexes, **3** and **4** displayed micromolar potency towards all of the cell lines tested, whereas **1** and **2** were relatively non-toxic. The potency of **3** and **4** towards CSC-enriched HMLER-shEcad cells was comparable to salinomycin, an established breast CSC-potent agent.[19] Notably, **3** indiscriminately killed HMLER-shEcad and HMLER cells, and exhibited 3.6- and 12.6-fold greater potency ($p < 0.05$, $n = 18$) for HMLER-shEcad cells over U2OS and HepG2 cells, respectively. As a measure of therapeutic potential, we determined the cytotoxicity of the most potent complex, **3** towards normal skin fibroblast GM07575 cells and mitochondria-rich human embryonic kidney HEK 293T cells. The complex, **3** was less potent towards GM07575 (IC_{50} value = 64.1 ± 0.4 μM, Figure S35) and HEK 293T cells (IC_{50} value = 22.1 ± 1.6 μM, Figure S36) than HMLER and HMLER-shEcad cells, indicating selective toxicity for breast bulk cancer cells and breast CSCs over non-tumorigenic cells. Markedly, **3** displayed 12-fold higher potency for HMLER-shEcad cells than GM07575 cells. Taken together, this suggests that **3** can potentially remove breast cancer cell populations in their entirety (bulk cancer cells and CSCs) with a single dose, with reduced toxicity towards bulk cancer and normal cells derived from other tissues.

The iridium(III) complexes remain intact in MEGM over the course of 24 h at 37 °C (Figures S27–S30), and thus cell toxicity is unlikely to result from the free ligands. Nevertheless, the cytotoxicity values of all of the ligands (2,2′-bipyridine, 4,4′-dimethyl-2,2′-bipyridine, 1,10-phenanthroline, 4,7-diphenyl-1,10-phenanthroline, and 1-methyl-2-(2-pyridyl)pyridinium hexafluorophosphate) were determined against HMLER-shEcad cells (72 h incubation, Figure S37, Table S6). The neutral ligands displayed micromolar potency against HMLER-shEcad cells, increasing in the following order; 2,2′-bipyridine < 4,4′-dimethyl-2,2′-bipyridine < 4,7-diphenyl-1,10-phenanthroline < 1,10-phenanthroline. Interestingly this trend is similar to that observed for the corresponding iridium(III) complexes, **1**–**4** against HMLER-shEcad cells. The positively charged ligand, 1-methyl-2-(2-pyridyl)pyridinium hexafluorophosphate was non-toxic towards HMLER-shEcad cells (IC_{50} < 100 μM).

The capability of **1**–**4** to inhibit spheroid formation from single-cell suspensions of CSC-enriched HMLER-shEcad cells was investigated using the mammospheres formation assay.[21] This method provides a reliable measure of CSC potency and in vivo potential. The treatment of **3** (at a non-lethal dose, IC_{20} value for 5 days) to single-cell suspensions of HMLER-shEcad cells dramatically reduced the number and size of mammospheres formed, comparable to salinomycin (Figure 2 and Figure S38). Dosage with **1**, **2**, and **4** (at a non-lethal dose, IC_{20}

Table 2. IC_{50} values of **1**–**4**, against U2OS, HepG2, HMLER, and HMLER-shEcad cells, and HMLER-shEcad mammospheres.

Cmpnd	U2OS IC_{50} [μM]	HepG2 IC_{50} [μM]	HMLER IC_{50} [μM]	HMLER-shEcad IC_{50} [μM]	Mammosphere IC_{50} [μM]
1	> 100	> 100	> 100	> 100	> 133
2	> 100	> 100	52.5 ± 3.7	64.4 ± 0.1	> 133
3	18.5 ± 3.0	65.4 ± 4.8	5.4 ± 0.3	5.2 ± 0.1	21.0 ± 0.2
4	37.5 ± 0.4	34.4 ± 0.3	9.1 ± 0.3	14.3 ± 1.8	> 133
salinomycin	n.d.	n.d.	11.4 ± 0.4[a]	4.2 ± 0.4[a]	18.5 ± 1.5[a]

[a] Taken from reference [20]. n.d. = not determined.

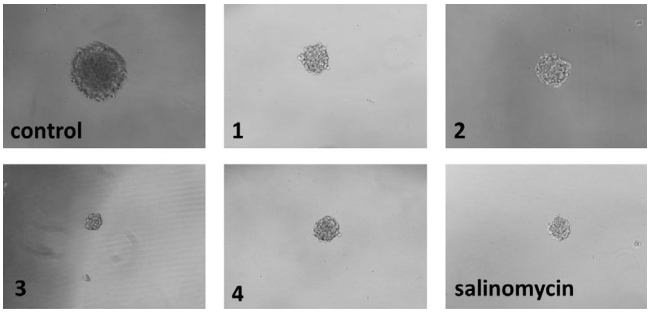

Figure 2. Representative bright-field images (×10) of the mammospheres in the absence and presence of **1**–**4** and salinomycin at their respective IC_{20} values.

value for 5 days) did not significantly affect the number of mammospheres formed; however, the size of mammospheres formed was markedly reduced (Figure 2 and Figure S38). To investigate the effect of **1**–**4** on mammosphere viability, the colorimetric resazurin-based reagent, TOX8 was used. Only the 1,10-phenanthroline-bearing complex **3** exhibited mammosphere potency, with an IC_{50} value (21.0 ± 0.2 μM) similar to salinomycin (18.5 ± 1.5 μM) under identical conditions (Figure S39). Given the cytotoxicity data in HMLER-shEcad monolayer systems (Table 2), it was unsurprising that **1**, **2**, and **4** displayed low mammosphere potency (IC_{50} > 133 μM) (Figure S39).

CSC uptake was determined by dosing HMLER-shEcad cells with **1**–**4** (10 μM for 16 h at 37 °C) and measuring the iridium content by ICP-MS (Figure S40). The iridium(III) complexes, **1**–**4** were readily taken up by HMLER-shEcad cells, with whole cell uptake ranging from 44.5 ± 0.1 ppb of Ir/million cells for **2** to 163.6 ± 1.3 ppb of Ir/million cells for **4**. To determine if CSC uptake was temperature dependent (and thereby active or passive), identical studies were conducted at 4 °C. HMLER-shEcad cells incubated with **1**–**4** (10 μM for 16 h at 4 °C) showed a significant decrease in uptake for **1** and **4** but not **2** and **3** (Figure S40). This indicates that the mechanism of CSC uptake is active for **1** and **4**, and passive for **2** and **3**. It should be noted that the iridium(III) complexes contain different polypyridyl ligands (2,2′-bipyridine, 4,4′-dimethyl-2,2′-bipyridine, 1,10-phenanthroline, or 4,7-diphenyl-1,10-phenanthroline). Thus, although the structural differences between **1**–**4** is subtle, their biological properties (such as cellular uptake pathway) can be drastically different. The varying modes of CSC uptake for **1**–**4** could be partly responsible for the lack of correlation between cellular uptake and lipophilicity or CSC cytotoxicity. To determine the CSC localization of **3** (the most effective complex within the iridium(III) series) fluorescence microscopy studies were performed. Co-treatment of HMLER-shEcad cells with the green-emitting iridium(III) complex **3** (10 μM for 24 h) and MitoTracker Deep Red FM (100 nM for 30 min), revealed a high level of overlap (Figure S41) suggesting that **3** localises in CSC mitochondria. The quality of the microscopy images was somewhat compromised by the reduced lifetime (0.80 μs) and quantum yield, Φ (4.7%) of **3** in phenol-free MEGM cell media (Figures S42 and S43). The imaging studies suggests that **3** can potentially cause mitochondrial dysfunction in CSCs.

Mitochondrial damage can lead to detrimental effects on mitochondrial metabolism and mitochondrial membrane potential.[22] The ability of **3** to inhibit cytochrome c oxidase, an enzyme responsible for reducing molecular oxygen to water in the respiratory electron transport chain, was determined. HMLER-shEcad cells dosed with **3** (10 μM for 24 h) displayed a significant decrease (45%, $p < 0.01$) in cytochrome c oxidase activity compared to control cells (Figure 3A), signifying mitochondrial respiration inhibition. Control studies with potassium cyanide (5–10 mM for 10 min), an established cytochrome c oxidase inhibitor, also showed considerable inhibition (Figure 3A). The integrity of the mitochondrial membrane potential of HMLER-shEcad cells upon treatment with **3** was probed

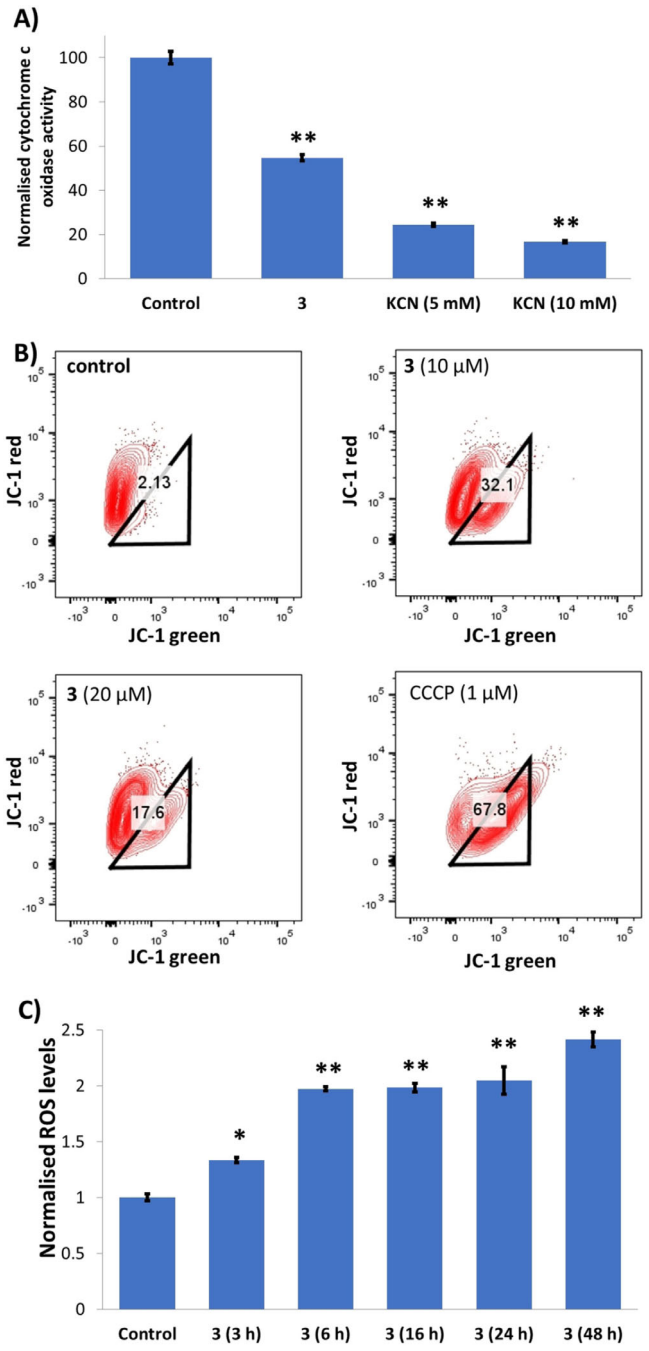

Figure 3. (A) Normalised cytochrome c oxidase activity in HMLER-shEcad cells treated with **3** (10 μM for 24 h) and KCN (5–10 mM for 10 min). Error bars = SD and Student t-test, ** = $p < 0.01$. (B) Representative 2D plots displaying the fluorescence emitted by JC-1 aggregates (red) and JC-1 monomers (green) by untreated HMLER-shEcad cells (top left), and HMLER-shEcad cells treated with **3** (10 μM for 24 h, top right), **3** (20 μM for 24 h, bottom left) and carbonyl cyanide *m*-chlorophenyl hydrazone (CCCP) (1 μM for 24 h, bottom right). (C) Normalised ROS activity in untreated HMLER-shEcad cells (control) and HMLER-shEcad cells treated with **3** (10 μM for 3–48 h). Error bars represent standard deviations and Student t-test, * = $p < 0.05$, ** = $p < 0.01$.

using the JC-1 assay. HMLER-shEcad cells incubated with **3** (10–20 μM for 24 h) showed up to 30% increase in the population of cells with depolarised mitochondrial membrane com-

pared to untreated control cells (Figure 3B). A similar, but more pronounced effect was observed for HMLER-shEcad cells dosed with carbonyl cyanide *m*-chlorophenyl hydrazone (CCCP) (1 μM for 24 h), a well-known mitochondrial membrane depolarizer (Figure 3B).

Disruption of regular mitochondrial processes can lead to an increase in intracellular ROS levels.[23] The ROS levels in untreated HMLER-shEcad cells and **3**-dosed (10 μM) HMLER-shEcad cells was measured using 6-carboxy-2′,7′-dichlorodihydrofluorescein diacetate, a ROS indicator, over the course of 48 h. As depicted in Figure 3C, **3** steadily increases ROS levels from 3 h (33% increase) to 48 h (141% increase). Similar time-dependent ROS generation has been reported for other mitochondrial-targeting agents. Control studies with HMLER-shEcad cells dosed with H_2O_2 (100 μM for 3–48 h) also showed an increase in ROS levels (up to 2.3-fold) (Figure S44). Cell viability studies in the presence of NAC (2.5 mM, 72 h), a ROS scavenger, showed that the potency of **3** towards HMLER-shEcad cells decreased significantly (IC_{50} value increased from 5.2 ± 0.1 μM to 15.1 ± 0.8 μM, $p < 0.05$) (Figure S45). This indicates that **3**-mediated CSC death is related to intracellular ROS generation. Mitochondrial dysfunction and ROS elevation can trigger intrinsic apoptosis, and thus an increase in the expression of active executioner caspases.[24] Immunoblotting studies showed that HMLER-shEcad cells treated with **3** (2.5, 5, and 10 μM for 72 h) expressed higher levels of cleaved caspase-3 and -7 than control cells, indicative of caspase-dependent apoptosis (Figure S46). Cytotoxicity studies in the presence of *z*-VAD-FMK (5 μM), a potent peptide-based apoptosis inhibitor, showed that the potency of **3** towards HMLER-shEcad cells decreased significantly (IC_{50} value increased from 5.2 ± 0.1 μM to 8.2 ± 0.2 μM, $p < 0.05$) (Figure S47). This confirms that **3** induces caspase-dependent CSC death.

In summary, we report a series of CSC-potent, iridium(III) complexes with high overall charge and mitochondrial targeting capabilities. The 1,10-phenanthroline-bearing complex **3** exhibited equal potency (in the micromolar range) towards bulk breast cancer cells and breast CSCs, implying that it could potentially remove heterogeneous breast cancer populations with a single dose. Mechanistic studies show that **3** enters breast CSCs, inhibits cytochrome c oxidase activity, promotes mitochondrial membrane depolarisation, elevates intracellular ROS, and triggers caspase-dependent apoptosis. This study, highlights the expanding potential of mitochondrial-targeting agents as anti-CSC agents and opens the door for the development of other iridium(III) complexes as CSC-active mitochondriotropics. Furthermore, in light of the findings reported in this manuscript, the anti-CSC potential of mitochondrial targeting iridium(III) complexes previously reported in the literature should be determined as they could provide promising anti-CSC leads.

Acknowledgements

K.L. and A.E. are supported by a KCL Ph.D. scholarship. K.S. thanks the Leverhulme Trust for funding (ECF-2014-178). C.L. thanks the Natural Science Foundation of China (Grant No.21401078) for financial support. We are grateful to Prof. Robert Weinberg (Whitehead Institute, MIT) for providing the cell lines used in this study. We thank Prof. Fiona Watt for insightful discussions on the biological studies.

Conflict of interest

The authors declare no conflict of interest.

Keywords: bioinorganic chemistry · cancer · cyclometallation · iridium · mitochondria

[1] a) L. V. Nguyen, R. Vanner, P. Dirks, C. J. Eaves, *Nat. Rev. Cancer* **2012**, *12*, 133–143; b) M. Dean, T. Fojo, S. Bates, *Nat. Rev. Cancer* **2005**, *5*, 275–284.

[2] a) J. Marx, *Science* **2007**, *317*, 1029–1031; b) D. R. Pattabiraman, R. A. Weinberg, *Nat. Rev. Drug Discovery* **2014**, *13*, 497–512; c) Y. Yu, G. Ramena, R. C. Elble, *Front. Biosci.* **2012**, *E4*, 1528–1541.

[3] a) L. N. Abdullah, E. K. Chow, *Clin. Transl. Med.* **2013**, *2*, 3; b) J. Kaiser, *Science* **2015**, *347*, 226–229; c) K. Rycaj, D. G. Tang, *Int. J. Radiat. Biol.* **2014**, *90*, 615–621.

[4] a) K. Chen, Y.-h. Huang, J.-l. Chen, *Acta. Pharmacol. Sin.* **2013**, *34*, 732–740; b) X. Ning, J. Shu, Y. Du, Q. Ben, Z. Li, *Cancer Biol. Ther.* **2013**, *14*, 295–303.

[5] I. S. Song, J. Y. Jeong, S. H. Jeong, H. K. Kim, K. S. Ko, B. D. Rhee, N. Kim, J. Han, *World J. Stem Cells* **2015**, *7*, 418–427.

[6] R. Lamb, G. Bonuccelli, B. Ozsvari, M. Peiris-Pages, M. Fiorillo, D. L. Smith, G. Bevilacqua, C. M. Mazzanti, L. A. McDonnell, A. G. Naccarato, M. Chiu, L. Wynne, U. E. Martinez-Outschoorn, F. Sotgia, M. P. Lisanti, *Oncotarget* **2015**, *6*, 30453–30471.

[7] K. Laws, G. Bineva-Todd, A. Eskandari, C. Lu, N. O'Reilly, K. Suntharalingam, *Angew. Chem. Int. Ed.* **2018**, *57*, 287–291; *Angew. Chem.* **2018**, *130*, 293–297.

[8] C. Rathi, B. Meibohm, *Pharmacokinetics of Peptides and Proteins* in *Reviews in Cell Biology and Molecular Medicine*, **2015**.

[9] Z. Liu, P. J. Sadler, *Acc. Chem. Res.* **2014**, *47*, 1174–1185.

[10] a) J. M. Hearn, I. Romero-Canelon, B. Qamar, Z. Liu, I. Hands-Portman, P. J. Sadler, *ACS Chem. Biol.* **2013**, *8*, 1335–1343; b) Z. Liu, A. Habtemariam, A. M. Pizarro, S. A. Fletcher, A. Kisova, O. Vrana, L. Salassa, P. C. Bruijnincx, G. J. Clarkson, V. Brabec, P. J. Sadler, *J. Med. Chem.* **2011**, *54*, 3011–3026; c) Z. Liu, I. Romero-Canelon, B. Qamar, J. M. Hearn, A. Habtemariam, N. P. Barry, A. M. Pizarro, G. J. Clarkson, P. J. Sadler, *Angew. Chem. Int. Ed.* **2014**, *53*, 3941–3946; *Angew. Chem.* **2014**, *126*, 4022–4027; d) S. J. Lucas, R. M. Lord, R. L. Wilson, R. M. Phillips, V. Sridharan, P. C. McGowan, *Dalton Trans.* **2012**, *41*, 13800–13802; e) S. Wirth, C. J. Rohbogner, M. Cieslak, J. Kazmierczak-Baranska, S. Donevski, B. Nawrot, I. P. Lorenz, *J. Biol. Inorg. Chem.* **2010**, *15*, 429–440; f) J. M. Hearn, G. M. Hughes, I. Romero-Canelon, A. F. Munro, B. Rubio-Ruiz, Z. Liu, N. O. Carragher, P. J. Sadler, *Metallomics* **2018**, *10*, 93–107; g) M. Gras, B. Therrien, G. Süss-Fink, A. Casini, F. Edafe, P. J. Dyson, *J. Organomet. Chem.* **2010**, *695*, 1119–1125.

[11] a) A. Wilbuer, D. H. Vlecken, D. J. Schmitz, K. Kraling, K. Harms, C. P. Bagowski, E. Meggers, *Angew. Chem. Int. Ed.* **2010**, *49*, 3839–3842; *Angew. Chem.* **2010**, *122*, 3928–3932; b) A. Kastl, A. Wilbuer, A. L. Merkel, L. Feng, P. Di Fazio, M. Ocker, E. Meggers, *Chem. Commun.* **2012**, *48*, 1863–1865.

[12] a) D. L. Ma, S. Lin, W. Wang, C. Yang, C. H. Leung, *Chem. Sci.* **2017**, *8*, 878–889; b) K. K.-W. Lo, K. Y. Zhang, *RSC Adv.* **2012**, *2*, 12069–12083.

[13] a) R. Gao, D. G. Ho, B. Hernandez, M. Selke, D. Murphy, P. I. Djurovich, M. E. Thompson, *J. Am. Chem. Soc.* **2002**, *124*, 14828–14829; b) S. Moromizato, Y. Hisamatsu, T. Suzuki, Y. Matsuo, R. Abe, S. Aoki, *Inorg. Chem.* **2012**, *51*, 12697–12706.

[14] R. Cao, J. Jia, X. Ma, M. Zhou, H. Fei, *J. Med. Chem.* **2013**, *56*, 3636–3644.

[15] a) V. Venkatesh, R. Berrocal-Martin, C. J. Wedge, I. Romero-Canelon, C. Sanchez-Cano, J.-l. Song, J. P. C. Coverdale, P. Zhang, G. J. Clarkson, A.

Habtemariam, S. W. Magennis, R. J. Deeth, P. J. Sadler, *Chem. Sci.* **2017**, *8*, 8271 – 8278; b) K. Qiu, Y. Liu, H. Huang, C. Liu, H. Zhu, Y. Chen, L. Ji, H. Chao, *Dalton Trans.* **2016**, *45*, 16144 – 16147; c) K. Xiong, Y. Chen, C. Ouyang, R.-L. Guan, L.-N. Ji, H. Chao, *Biochimie* **2016**, *125*, 186 – 194; d) L. He, K.-N. Wang, Y. Zheng, J.-J. Cao, M.-F. Zhang, C.-P. Tan, L.-N. Ji, Z.-W. Mao, *Dalton Trans.* **2018**, *47*, 6942 – 6953; e) C. Caporale, C. A. Bader, A. Sorvina, K. D. M. MaGee, B. W. Skelton, T. A. Gillam, P. J. Wright, P. Raiteri, S. Stagni, J. L. Morrison, S. E. Plush, D. A. Brooks, M. Massi, *Chem. Eur. J.* **2017**, *23*, 15666 – 15679.

[16] R. W. Horobin, S. Trapp, V. Weissig, *J. Controlled Release* **2007**, *121*, 125 – 136.

[17] a) B. J. Coe, M. Helliwell, J. Raftery, S. Sanchez, M. K. Peers, N. S. Scrutton, *Dalton Trans.* **2015**, *44*, 20392 – 20405; b) B. J. Coe, M. Helliwell, S. Sanchez, M. K. Peers, N. S. Scrutton, *Dalton Trans.* **2015**, *44*, 15420 – 15423.

[18] R. A. J. Smith, C. M. Porteous, A. M. Gane, M. P. Murphy, *Proc. Natl. Acad. Sci. USA* **2003**, *100*, 5407 – 5412.

[19] P. B. Gupta, T. T. Onder, G. Jiang, K. Tao, C. Kuperwasser, R. A. Weinberg, E. S. Lander, *Cell* **2009**, *138*, 645 – 659.

[20] a) C. Lu, K. Laws, A. Eskandari, K. Suntharalingam, *Dalton Trans.* **2017**, *46*, 12785 – 12789; b) J. N. Boodram, I. J. McGregor, P. M. Bruno, P. B. Cressey, M. T. Hemann, K. Suntharalingam, *Angew. Chem. Int. Ed.* **2016**, *55*, 2845 – 2850; *Angew. Chem.* **2016**, *128*, 2895 – 2900.

[21] G. Dontu, W. M. Abdallah, J. M. Foley, K. W. Jackson, M. F. Clarke, M. J. Kawamura, M. S. Wicha, *Genes Dev.* **2003**, *17*, 1253 – 1270.

[22] X. Wang, *Genes Dev.* **2001**, *15*, 2922 – 2933.

[23] a) M. P. Murphy, *Biochem. J.* **2009**, *417*, 1 – 13; b) C. H. Wang, S. B. Wu, Y. T. Wu, Y. H. Wei, *Exp. Biol. Med.* **2013**, *238*, 450 – 460.

[24] S. W. G. Tait, D. R. Green, *Nat. Rev. Mol. Cell Biol.* **2010**, *11*, 621 – 632.

[25] CCDC 1836118 (**2**) contains the supplementary crystallographic data for this paper. These data are provided free of charge by The Cambridge Crystallographic Data Centre.

Manuscript received: July 10, 2018
Revised manuscript received: July 26, 2018
Accepted manuscript online: July 27, 2018
Version of record online: ■■ ▮▮, 0000

COMMUNICATION

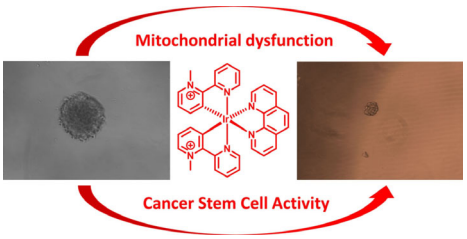

Iridium mitochondriotropics: A series of iridium(III) complexes bearing polypridyl and charged 1-methyl-2-(2-pyridyl)pyridinium ligands, is reported and their anti-cancer stem cell properties are described in detail. The highly charged, lipophilic compounds are shown to kill breast cancer stem cells by disrupting mitochondrial membrane potential and mitochondrial respiration.

Antitumor Agents

*K. Laws, A. Eskandari, C. Lu, K. Suntharalingam**

■■ – ■■

Highly Charged, Cytotoxic, Cyclometalated Iridium(III) Complexes as Cancer Stem Cell Mitochondriotropics